Int. J. Solids Structures Vol. 30, No. 21, pp. 2953–2969, 1993
Printed in Great Britain

0020-7683/93 $6.00+.00

CHAOTIC MOTION OF A PARAMETRICALLY FORCED SIMPLE PENDULUM

JIIN-PO YEH
Department of Civil Engineering, Kaohsiung Polytechnic Institute, 1, Section 1, Hsueh-Cheng Road, Ta-Hsu Hsiang, Kaohsiung County, Taiwan, R.O.C.

(*Received* 2 *November* 1992; *in revised form* 19 *April* 1993)

Abstract—This paper describes the behavior of a simple pendulum with support in a steady and rather slow circular motion in a vertical plane. The governing equation of this model is nonlinear, and its motion is about the direction of gravity. In the equation of motion, there are three parameters, which are related to the radius and angular velocity of the circular motion, the length of the pendulum and the damping constant. For some combinations of these parameters, this model is found to have chaotic motion by numerical integration.

This paper not only draws the time series and Poincaré map to show the characteristics of regular and chaotic motions, but also explores the feasibility of using the amplitude probability distribution by numerical method to diagnose whether the motion is chaotic. The effect of geometry and damping constant on the motion of the system is investigated. Furthermore, whether the Poincaré map and amplitude probability distribution depend sensitively on the initial conditions is also studied.

1. INTRODUCTION

A uniform physical pendulum whose support is in a steady and fast circular motion in a vertical plane was first investigated by Panayotidi and DiMaggio (1988). They dealt with the classical nonlinear dynamics regarding periodic motions. Afterwards, Yeh and DiMaggio (1991) probed both the periodic motion and chaotic motion of that model with and without damping. The chaotic motion was found to exist. This paper continues to work on a similar model, which is a simple pendulum whose support is in a steady and very slow circular motion. Because this model describes the behaviors of systems like the ferris wheel, the angle of oscillation is measured from the vertical line, instead of the radial line.

The purpose of this paper is to find the routes to chaos for systems with and without damping, to exhibit the characteristics of the chaotic motion found on the Poincaré map and the amplitude probability distribution, and to explore the effects of damping and the geometry of the system on the motion.

This paper is arranged as follows. Section 2 derives the equation of motion. The subsequent section describes how the Poincaré map and amplitude probability distribution are obtained. Section 4 introduces the Lyapunov exponents and fractal dimension. Numerical methods and results are given in Section 5. The conclusion is in Section 6 with a few remarks.

2. EQUATION OF MOTION

This paper considers a system like the ferris wheel with only one carriage. It can be modeled as in Fig. 1. Support A is in steady and very slow circular motion with a radius of R and angular velocity of Ω. M is the mass of the simple pendulum and L is its length. Suppose that the mass moment of inertia of the driving wheel F about the axis passing through the fixed point O is I_o and the damping of the simple pendulum is C_p. Let r be the position vector of B with respect to the fixed reference point O. The kinetic energy of the system is

$$\begin{aligned} T &= \tfrac{1}{2}M\dot{r}\cdot\dot{r}+\tfrac{1}{2}I_o\Omega^2 \\ &= \tfrac{1}{2}M[R^2\Omega^2+L^2\dot{\Phi}^2+2R\Omega L\dot{\Phi}\cos(\Phi-\Omega t)]+\tfrac{1}{2}I_o\Omega^2, \end{aligned} \tag{1}$$

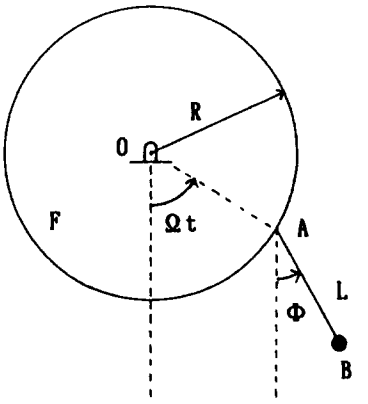

Fig. 1. Simple pendulum with support in low-speed circular motion.

where $\dot{r} = (\mathrm{d}r/\mathrm{d}t)$. Assume that the horizontal line passing through the point O in Fig. 1 is the datum for the potential energy. Accordingly, the potential energy of the system is

$$V = -Mg(R\cos\Omega t + L\cos\Phi). \tag{2}$$

Substituting eqns (1) and (2) into Lagrange's equation leads to the equation of motion

$$\ddot{\Phi} + \frac{C_p}{ML^2}\dot{\Phi} + \frac{R\Omega^2}{L}\sin(\Phi - \Omega t) + \frac{g}{L}\sin\Phi = 0. \tag{3}$$

Let $\tau = \Omega t$. Equation (3) can be changed to

$$\Phi'' + \frac{C_p}{ML^2\Omega}\Phi' + \frac{R}{L}\sin(\Phi - \tau) + \frac{g}{\Omega^2 L}\sin\Phi = 0, \tag{4}$$

where

$$\Phi'' = \frac{\mathrm{d}^2\Phi}{\mathrm{d}\tau^2} \quad \text{and} \quad \Phi' = \frac{\mathrm{d}\Phi}{\mathrm{d}\tau}.$$

For simplification, eqn (4) is written as

$$\Phi'' + C\Phi' + E\sin\Phi = D\sin(\tau - \Phi), \tag{5}$$

where

$$C = \frac{C_p}{ML^2\Omega}, \quad E = \frac{g}{\Omega^2 L} \quad \text{and} \quad D = \frac{R}{L}.$$

Parameters C, D and E are all dimensionless.

3. POINCARE MAPS AND AMPLITUDE PROBABILITY DISTRIBUTION

3.1. *Poincaré maps*

If a nonautonomous system, whose governing equation is $\Phi'' = f(\Phi', \Phi, \tau)$ has a very long period or is nonperiodic, the projection of its trajectory onto the phase plane of (Φ', Φ) must be very complicated, from which it's very difficult to get information. In chaotic dynamics, the Poincaré map is often used to simplify the picture on the phase plane. If the

period of the driving function in the governing function is T, then the rule for the Poincaré map is usually to sample the points at times when $\tau_n = nT + \tau_o$, where n is a non-negative integer. Depending on the types of motion, the Poincaré map has the following patterns:

(1) a set of q points, if $\Phi(\tau + s\tau) = \Phi(\tau)$ in which s is a rational number q/p;
(2) a closed curve (or closed curves), if $\Phi(\tau + s\tau) = \Phi(\tau)$ in which s is irrational;
(3) fractal collection of points, if the motion can't be expressed in the above two forms.

3.2. *Amplitude probability distribution*

This paper uses a direct method to find the amplitude probability distribution. First, divide the interval between the largest and smallest amplitudes of the motion equally into as many subintervals as possible. Secondly, find which subintervals each iteration belongs to from the result of the numerical integration. Finally, divide the number of iterations in each subinterval by the total number of iterations. The more iterations the numerical integration has, the more accurate the probability distribution is.

If the motion of the system is periodic, some amplitudes will appear repeatedly and fall into the same subinterval as the numerical integration proceeds, but some subintervals never catch any iterations. Therefore, its amplitude probability distribution is discrete. If the motion is quasi-periodic or chaotic, every subinterval will catch iterations, and its amplitude probability distribution is continuous.

4. LYAPUNOV EXPONENTS AND FRACTAL DIMENSION

Suppose that there is a small circle of radius $d(\tau_n)$ corresponding to different initial conditions at time τ_n. At a later time $\tau_n + \Delta_\tau$, these set of points evolve into an ellipse with major principal axis $d_1(\tau_{n+1})$ and minor principal axis $d_2(\tau_{n+1})$, as shown in Fig. 2. The lengths of these two axes are

$$d_1(\tau_{n+1}) = d(\tau_n) 2^{\lambda_{1n}\Delta_\tau}, \tag{6}$$

$$d_2(\tau_{n+1}) = d(\tau_n) 2^{\lambda_{2n}\Delta_\tau}, \tag{7}$$

where λ_{1n} and λ_{2n} are Lyapunov exponents to measure the variation of these two axes during the time interval Δ_τ. The Lyapunov exponents λ_1 and λ_2 are obtained by averaging the Lyapunov exponents found at every interval Δ_τ throughout the whole time history. That is

$$\lambda_i = \lim_{N\to\infty} \frac{1}{\tau - \tau_o} \sum_{n=0}^{N-1} \log_2 \frac{d_i(\tau_{n+1})}{d_i(\tau_n)}, \quad i = 1, 2 \tag{8}$$

and $\lambda_1 > \lambda_2$. The system is defined as chaotic if $\lambda_1 > 0$, quasi-periodic if $\lambda_1 = 0$ or periodic if $\lambda_1 < 0$.

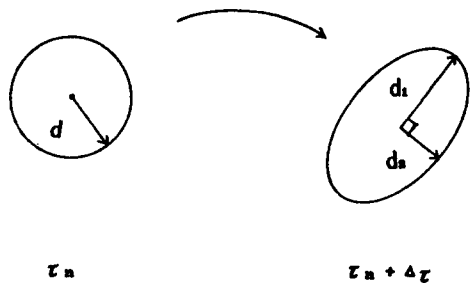

Fig. 2. Evolution of a small circle into an ellipse.

For a damped system, the points on the Poincaré map are not distributed uniformly, so its dimension is called a fractal dimension. There are a number of means to measure the dimension of a set of points, such as capacity dimension, information dimension, pointwise dimension, Lyapunov dimension, etc., discussed by Farmer *et al.* (1983) and Frederickson *et al.* (1983). Lyapunov dimension is chosen to find the dimension of a set of points in this paper. Its formula is

$$d_1 = 1 - \lambda_1/\lambda_2. \tag{9}$$

Let the area of the initial circle in Fig. 2 be A_n and the evolved ellipse be A_{n+1}. Then

$$A_{n+1} = A_n 2^{(\lambda_{1n}+\lambda_{2n})\Delta_\tau}. \tag{10}$$

5. NUMERICAL METHODS AND RESULTS

5.1. *Numerical methods*

In this paper, the Runge–Kutta–Fehlberg method from Gerald and Wheatley (1984) is used to find solutions to the set of coupled ordinary differential equations. To find Φ and Φ', eqn (5) is first changed to

$$\Phi_1' = \Phi_2, \tag{11}$$

$$\Phi_2' = D\sin(\tau - \Phi_1) - C\Phi_2 - E\sin\Phi_1, \tag{12}$$

where $\Phi_1 = \Phi$. Because the period of Φ is 2π, Φ is restricted between $-\pi$ and π for simplification. To find the exponential growth of the principal axes in Fig. 2, eqns (11) and (12) are linearized to get two sets of variational equations. The first set for one of the two principal axes is

$$\delta\Phi_1' = \alpha_1' = \alpha_2 \tag{13}$$

$$\delta\Phi_2' = \alpha_2' = -[D\cos(\tau - \Phi_1) + E\cos\Phi_1]\alpha_1 - C\alpha_2. \tag{14}$$

The second set for the other principal axes is

$$\delta\Phi_1' = \beta_1' = \beta_2, \tag{15}$$

$$\delta\Phi_2' = \beta_2' = -[D\cos(\tau - \Phi_1) + E\cos\Phi_1]\beta_1 - C\beta_2. \tag{16}$$

Equations (11)–(16) are then solved simultaneously. The unit vectors **OP** of $(\alpha_1(0), \alpha_2(0))$ and **OQ** of $(\beta_1(0), \beta_2(0))$ in Fig. 3 are perpendicular to each other. At τ_1, $O \to O'$, $P \to P'$ and $Q \to Q'$, **OP**′ and **OQ**′ are not perpendicular to each other any more. Therefore, **OP**′ and **OQ**″, instead of **OQ**′, are chosen to measure the growth of the two principal axes. **OQ**″ is the component of **OQ**′ in the direction perpendicular to **OP**′. Since **OP**′ is free to follow the fast growth direction, substituting **OP** and **OP**′ into eqn (6) leads to λ_{1n}, while substituting **OQ** and **OQ**″ into eqn (7) leads to λ_{2n}. Before going to the next mapping, **OP**′ and **OQ**″ are normalized in order to make computation simple. According to eqn (8), λ_1 and λ_2 are finally found by averaging all the λ_{1n}s and λ_{2n}s.

5.2. *Numerical results*

The initial value of $(\Phi(0), \Phi'(0))$ is (0.0873, 0.0) in all calculations unless specified.

5.2.1. $C = 0.0$. The solutions to eqns (11) and (12) are obtained for $C = 0.0$, $1 \leqslant D \leqslant 10$ and $10 \leqslant E \leqslant 300$. The increment is 1 for D and 10 for E. When $E \geqslant 20$, the motion is quasi-periodic. The Poincaré map for $D = 1$ and $E = 10$ consists of two inter-

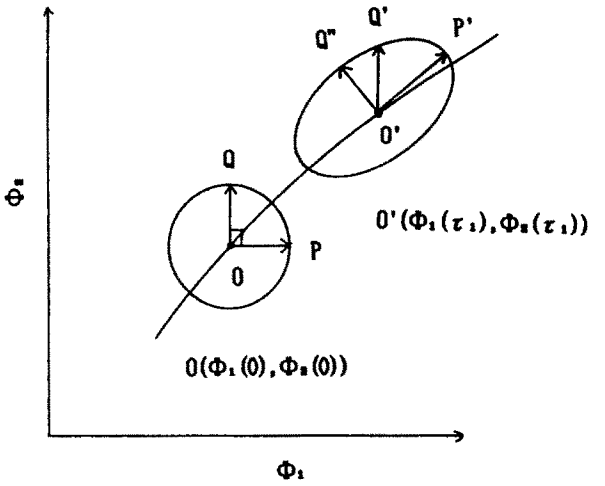

Fig. 3. Trajectory of the initial point O and the variation of the length of OP and OQ.

secting closed curves, as shown in Fig. 4(a). These two curves are generated by a single trajectory which jumps successively from one to the other. When D increases, they move further apart, as illustrated in Figs 4(b) and (c) which are for $D = 2$ and $D = 3$, respectively. In order to discover the route to chaos, the increment of D is decreased to 0.01 and E is fixed at 10. It is found that the system is still in quasi-periodic motion until D reaches 3.92. The time series and Poincaré map for $D = 3.92$ and $E = 10$ are shown in Figs 5(a) and (b), respectively, and Fig. 5(c) is its amplitude probability distribution. When $D = 3.93$, the motion becomes chaotic. Therefore, quasi-periodic route is the model for the system without damping to become chaotic. Figures 6(a) and (b) are the time series and Poincaré map, respectively, for $D = 4.0$ and $E = 10.0$. Since the system is undamped, no strange attractor appears on the Poincaré map. If the initial conditions are (0.1, 0.0), an identical Poincaré map is obtained, as shown in Fig. 7. If enough points are sampled, the points on the Poincaré map should appear to be uniformally distributed. Figure 8(a) is the amplitude probability distribution for $D = 4.0$ and $E = 10$, which is continuous as well. If the initial conditions are (0.1, 0.0), a different shape of amplitude probability distribution is found, as shown in Fig. 8(b). Hence, the amplitude probability distribution of chaotic motion is very sensitive to the initial conditions, but the Poincaré map is not. Although the amplitude probability distribution for both quasi-periodic and chaotic motion is continuous, there are still differences between them. The range of amplitude is always $-\pi \leqslant \Phi \leqslant \pi$ for chaotic motion, while it is smaller for quasi-periodic motion, as illustrated in Figs 5(c) and 8(a).

The Lyapunov exponents λ_1 and λ_2, $\lambda_1+\lambda_2$, and fractal dimension d_1 for $E = 10$ and $D = 3.93$, 5.0, 8.0 and 10.0 are listed in Table 1, from which it is found that $\lambda_1 = -\lambda_2$, $d_1 = 2$ and λ_1 becomes larger when D increases. According to eqn (10), the area of the circle of initial conditions remains unchanged because $\lambda_1+\lambda_2 = 0$.

5.2.2. $C = 0.1$. The solutions to eqns (11) and (12) are obtained for $C = 0.1$, $1 \leqslant D \leqslant 10$ and $10 \leqslant E \leqslant 300$. The increment is 1 for D and 10 for E. When $E = 10$ and

Table 1. Lyapunov exponents λ_1 and λ_2, $\lambda_1+\lambda_2$ and λ_1 for $C = 0.0$, $E = 10$ and $D = 3.93$, 5.0, 8.0 and 10.0

C	D	E	λ_1	λ_2	$\lambda_1+\lambda_2$	d_1
0.0	3.93	10.0	0.2122	−0.2122	0.0	2.0
0.0	5.0	10.0	0.2813	−0.2813	0.0	2.0
0.0	8.0	10.0	0.3484	−0.3484	0.0	2.0
0.0	10.0	10.0	0.3794	−0.3794	0.0	2.0

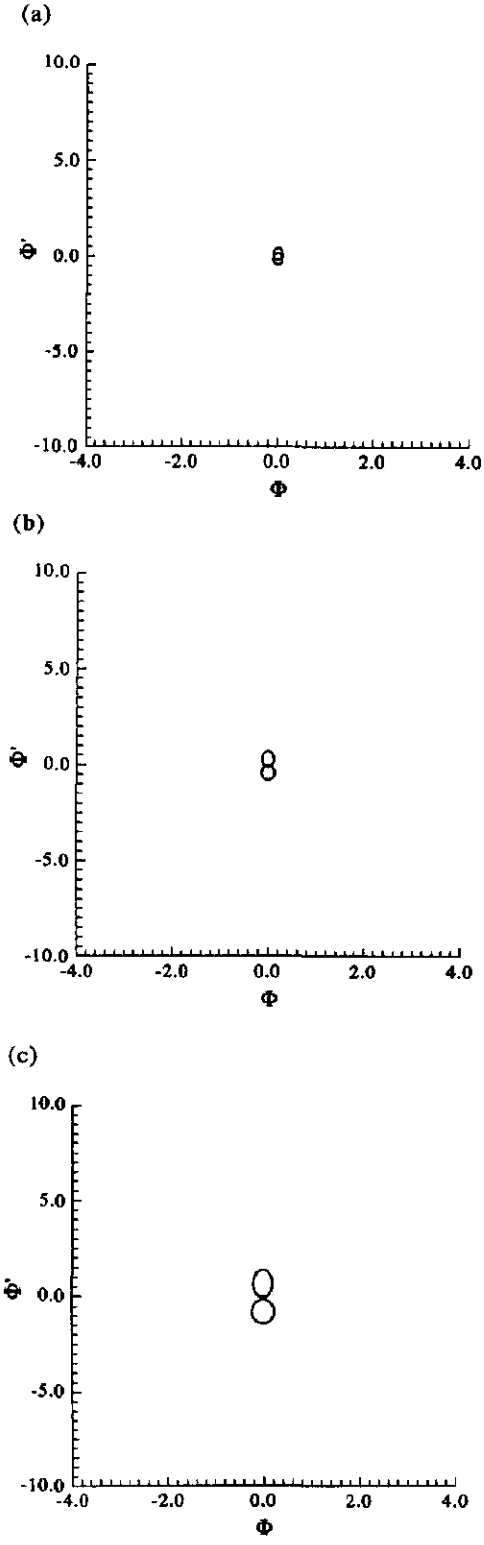

Fig. 4. Poincaré maps for initial conditions (0.0873, 0.0) and (a) $C = 0.0$, $D = 1$ and $E = 10$, (*b*) $C = 0.0$, $D = 2$ and $E = 10$, and (c) $C = 0.0$, $D = 3$ and $E = 10$.

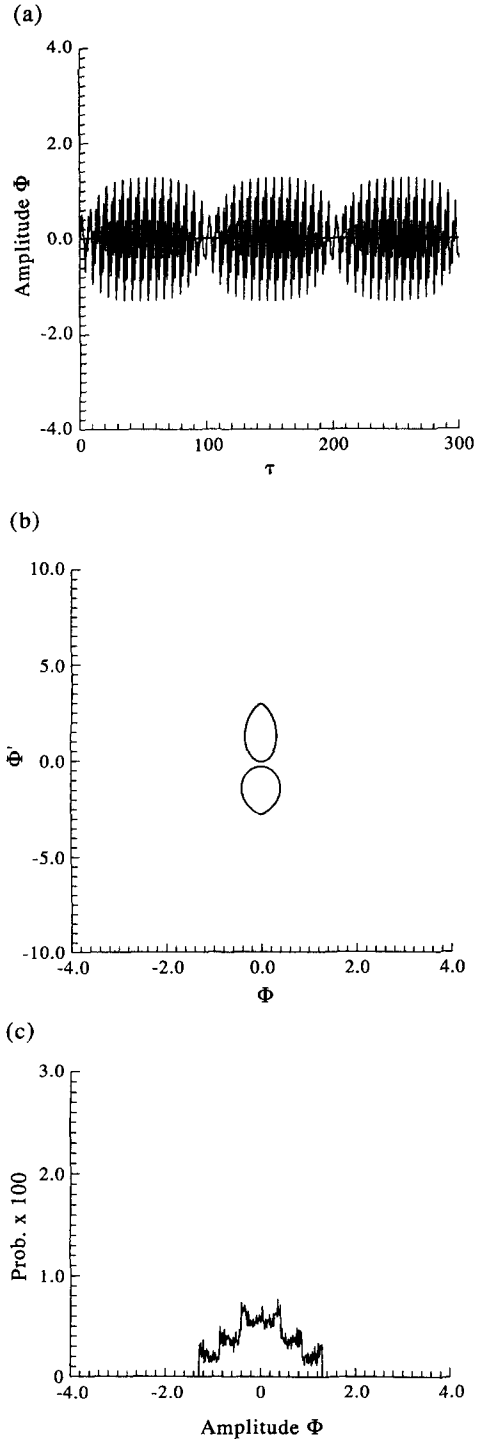

Fig. 5. (a) Time history, (b) Poincaré map, and (c) amplitude probability distribution for $C = 0.0$, $D = 3.92$, $E = 10$ and initial conditions (0.0873, 0.0).

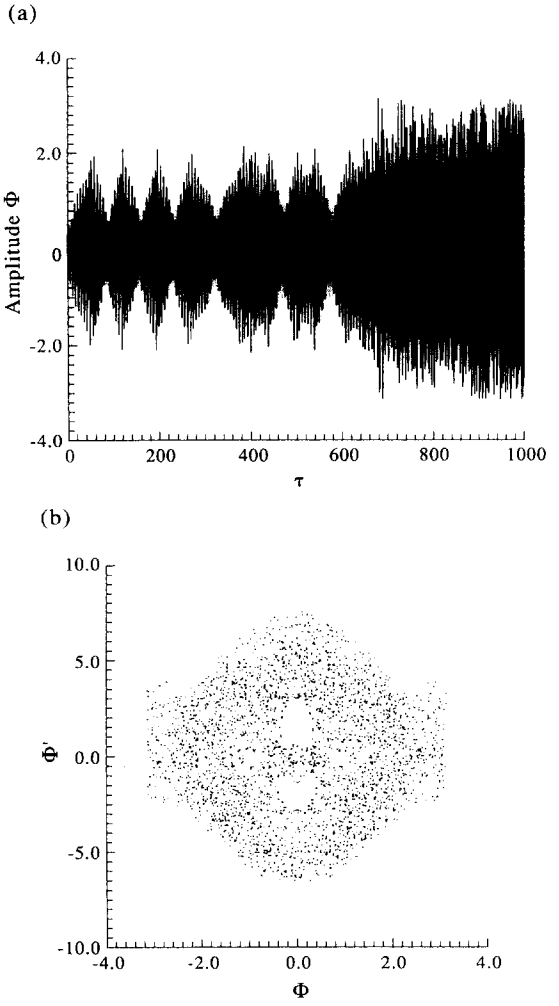

Fig. 6. (a) Time history and (b) Poincaré map for $C = 0.0$, $D = 4$, $E = 10$ and initial conditions (0.0873, 0.0).

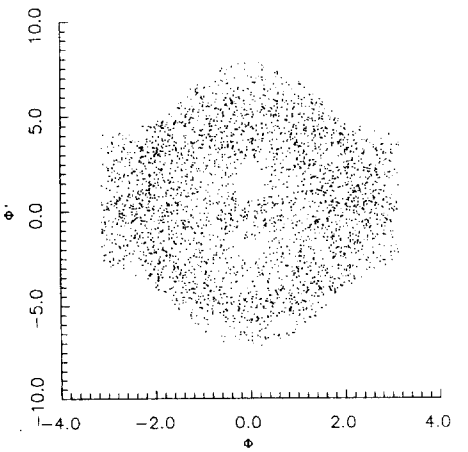

Fig. 7. Poincaré map for $C = 0.0$, $D = 4$, $E = 10$ and initial conditions (0.1, 0.0).

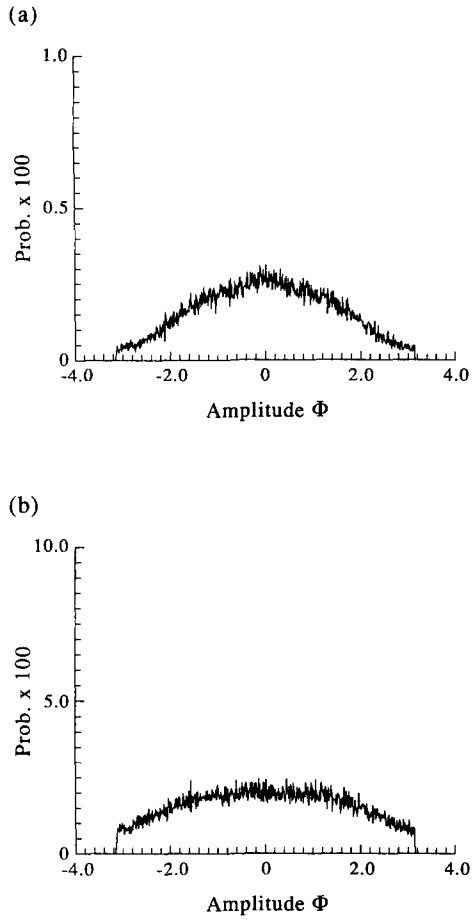

Fig. 8. Amplitude probability distribution for $C = 0.0$, $D = 4$, $E = 10$, and initial conditions (a) (0.0873, 0.0), and (b) (0.1, 0.0).

$1 \leqslant D \leqslant 6$, the motion is periodic and its Poincaré map consists of two points. Because the sample interval on the Poincaré map is π, the period of the motion is 2π. Figures 9(a), (b) and (c) show the Poincaré maps for $E = 10$ and $D = 2$, 4 and 6, respectively. From these maps, it can be seen that as D increases, the distance between these two points becomes larger and larger. This phenomenon is similar to the bifurcation diagram for the logistic equation by Jensen (1987). In order to understand how the motion becomes chaotic, the increment of D is decreased to 0.01 with E fixed at 10. As D increases above 6, the system bifurcates to periodic motion with twice the period of the previous oscillation as shown in Figs 10(a), (b) and (c) which are for $D = 6.1$, 6.3 and 6.31, respectively. The interval between the bifurcation points becomes smaller as the parameter D increases. When D reaches 6.33, the motion becomes chaotic. Hence the system becomes chaotic by the route of period-doubling. The amplitude probability distribution for periodic motion is discrete. Figure 11(a) is the time series and Fig. 11(b) is the amplitude probability distribution after transition for $D = 6$ and $E = 10$. Figures 12(a) and 12(b) are the time series and Poincaré map, respectively, for $D = 6.33$ and $E = 10$. If the initial conditions are (0.1, 0.0), an identical Poincaré map is obtained, as shown in Fig. 13. Fig. 14(a) is the amplitude probability distribution, for $D = 6.33$ and $E = 10$. Its range of amplitude is $-\pi$–π. If the initial conditions are (0.1, 0.0), a different shape of amplitude probability is found, as shown in Fig. 14(b). Therefore, the amplitude probability distribution of chaotic motion of the damped system is also very sensitive to the initial conditions, but the Poincaré map is not.

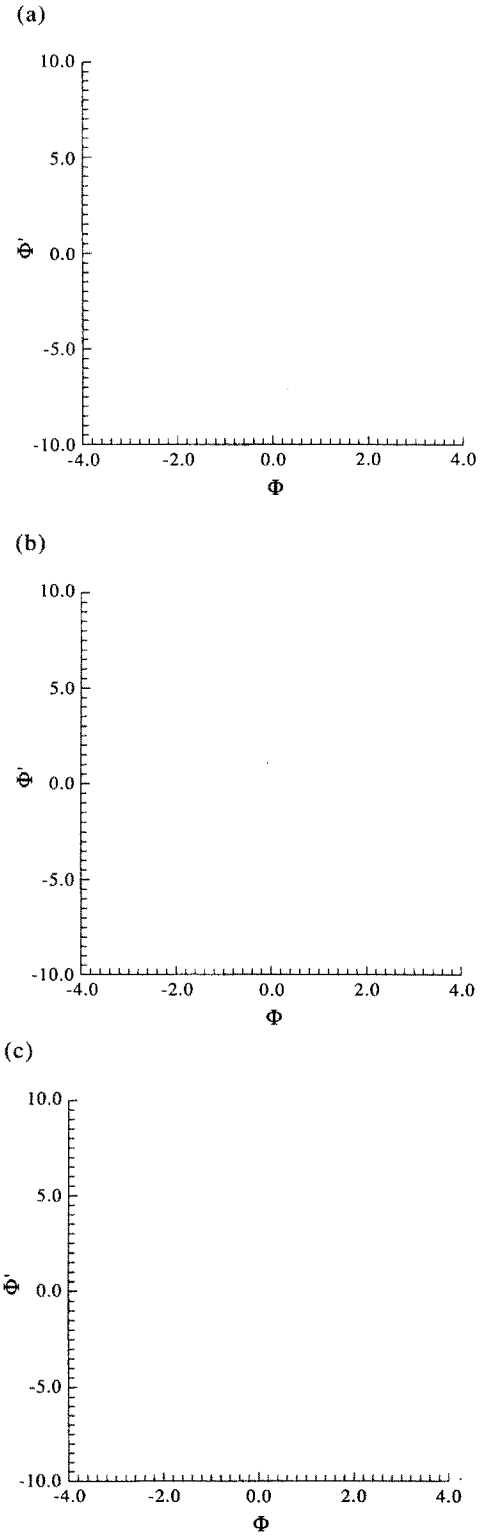

Fig. 9. Poincaré maps after transition for $C = 0.1$, $E = 10$, initial conditions (0.0873, 0.0) and (a) $D = 2$, (b) $D = 4$, and (c) $D = 6$.

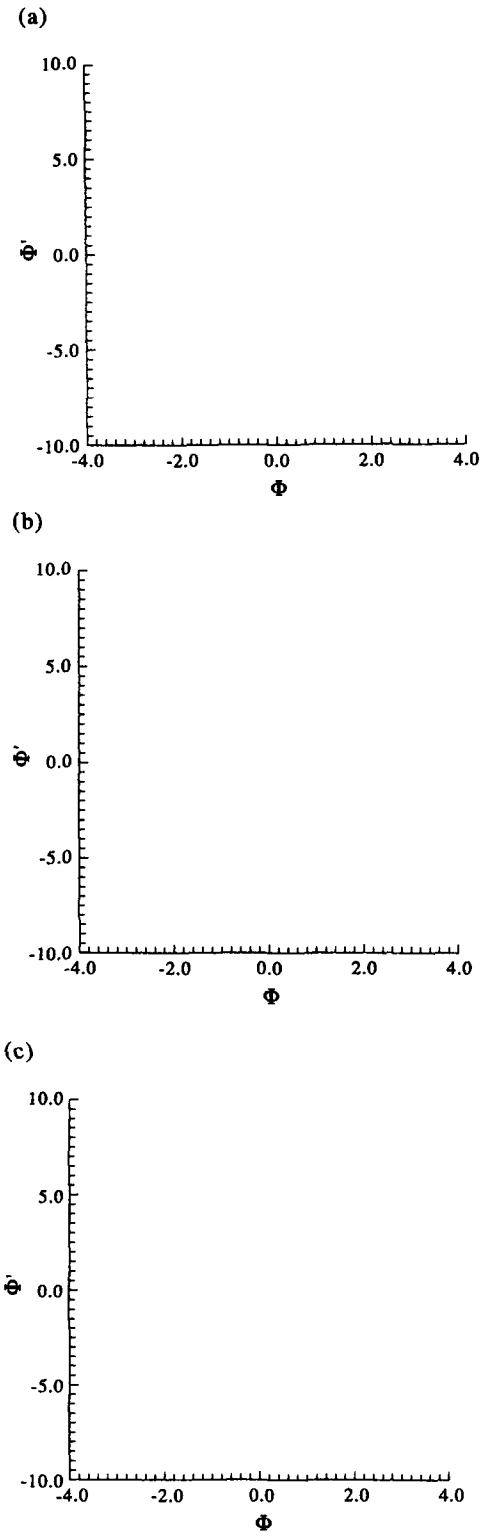

Fig. 10. Poincaré maps for $C = 0.1$, $E = 10$, initial conditions (0.0873, 0.0) and (a) $D = 6.1$, (b) $D = 6.3$, and (c) $D = 6.31$.

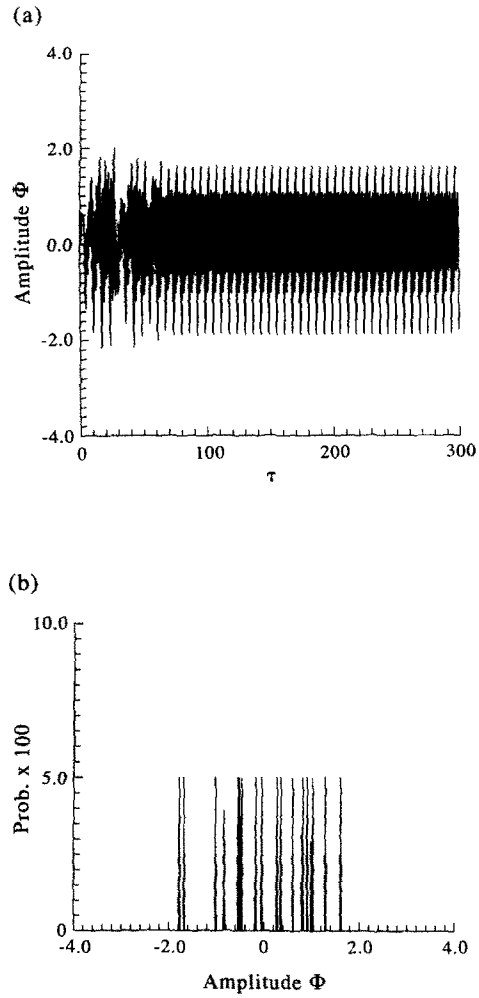

Fig. 11. (a) Time history and (b) amplitude probability distribution after transition for $C = 0.1$, $D = 6$, $E = 10$ and initial conditions (0.0873, 0.0).

Table 2 lists the Lyapunov exponents λ_1, λ_2, $\lambda_1+\lambda_2$ and fractal dimension d_l for $E = 10$ and $D = 6.33$, 8.0 and 10.0. Since $\lambda_1+\lambda_2 = -1.4427C$, according to Yeh and DiMaggio (1991), $\lambda_1+\lambda_2 = -0.1443$. Table 2 shows λ_1 and d_l become larger when D increases. Figures 12(b) and 15, which are the Poincaré maps for $C = 0.1$, $D = 10$ and $E = 10$, show that the larger D is, the bigger d_l is. Since the system has damping, d_l is between 1 and 2. When $E > 10$, the system becomes periodic again.

If C changes from 0.1 to 10 with an increment of 0.1, chaos only exists at $E = 10$ but begins to happen at larger D when C is larger. For example, if $C = 0.5$, chaos begins to happen at $D = 9$.

5.2.3. $D = 10$. Let D be fixed at 10. That is, the geometry is fixed. Change C from 0 to 1.0 with an increment of 0.1 and E from 10 to 300 with an increment of 10. It is found

Table 2. Lyapunov exponents λ_1 and λ_2, $\lambda_1+\lambda_2$ and λ_1 for $C = 0.1$, $E = 10$ and $D = 6.33$, 8.0 and 10.0

C	D	E	λ_1	λ_2	$\lambda_1+\lambda_2$	d_l
0.1	6.33	10.0	0.1053	−0.2496	−0.1443	1.421
0.1	8.0	10.0	0.1988	−0.3431	−0.1443	1.579
0.1	10.0	10.0	0.2495	−0.3938	−0.1443	1.633

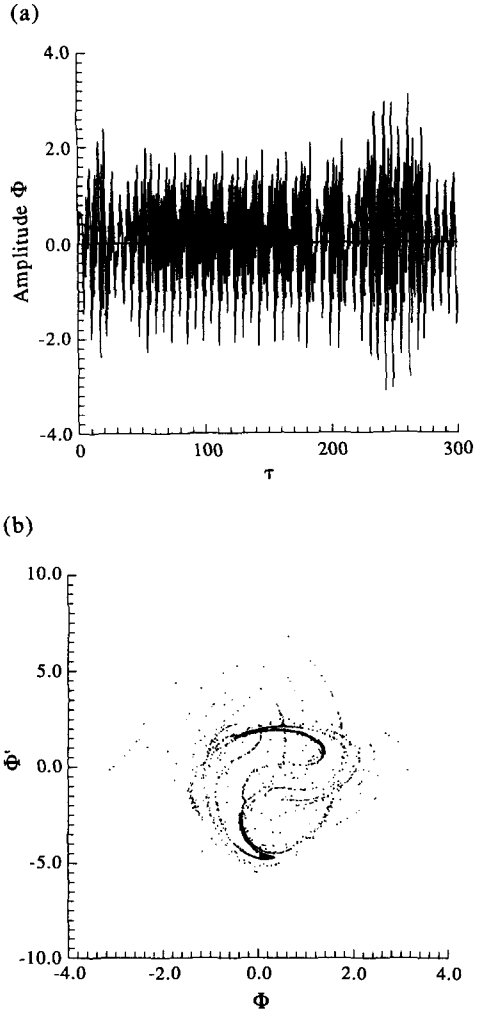

Fig. 12. (a) Time history and (b) Poincaré map for $C = 0.1$, $D = 6.33$, $E = 10$ and initial conditions (0.0873, 0.0).

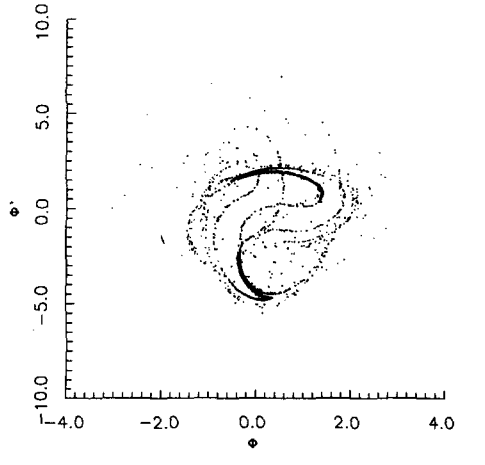

Fig. 13. Poincaré map for $C = 0.1$, $D = 6.33$, $E = 10$ and initial conditions (0.1, 0.0).

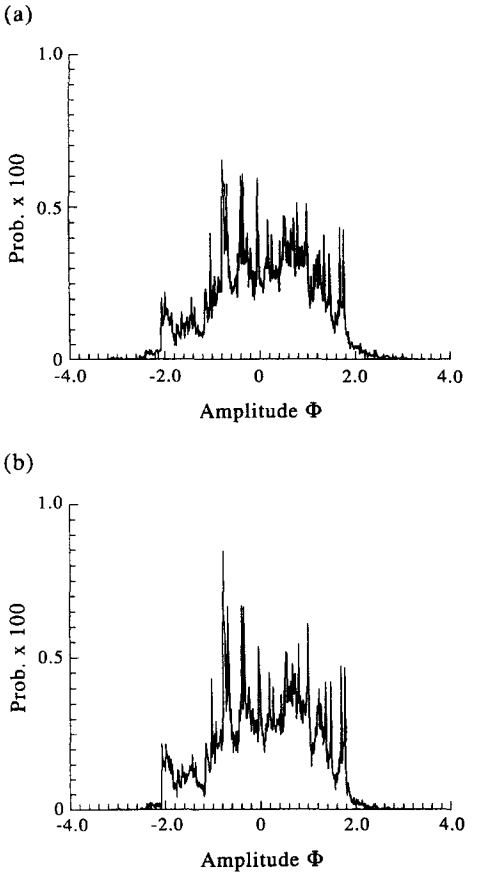

Fig. 14. Amplitude probability distribution for $C = 0.1$, $D = 6.33$, $E = 10$ and initial conditions (a) (0.0873, 0.0), and (b) (0.1, 0.0).

that chaos happens only at $E = 10$. The Lyapunov exponents λ_1, λ_2, $\lambda_1+\lambda_2$ and d_1 for $E = 10$ and $C = 0.0$, 0.2, 0.4, 0.6 and 0.8 are shown in Table 3. It is observed that when C increases, $\lambda_1+\lambda_2$ becomes more negative and d_1 becomes smaller. Since $\lambda_1+\lambda_2$ is negative, the area of the circle in Fig. 2 decreases as time increases. The effect of the damping on the fractal dimension can be seen in Figs 16(a), (b) and (c), which are the Poincaré maps for $D = 10$, $E = 10$ and $C = 0.4$, 0.6 and 0.8, respectively.

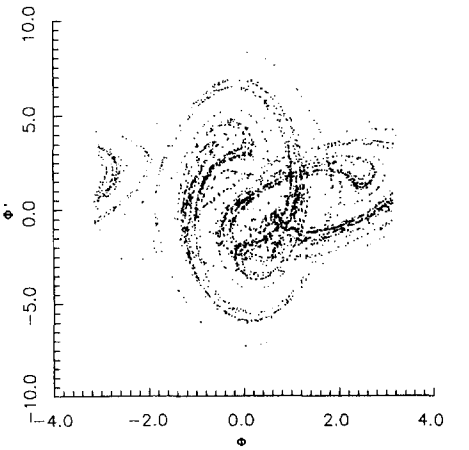

Fig. 15. Poincaré map for $C = 0.1$, $D = 10$, $E = 10$ and initial conditions (0.0873, 0.0).

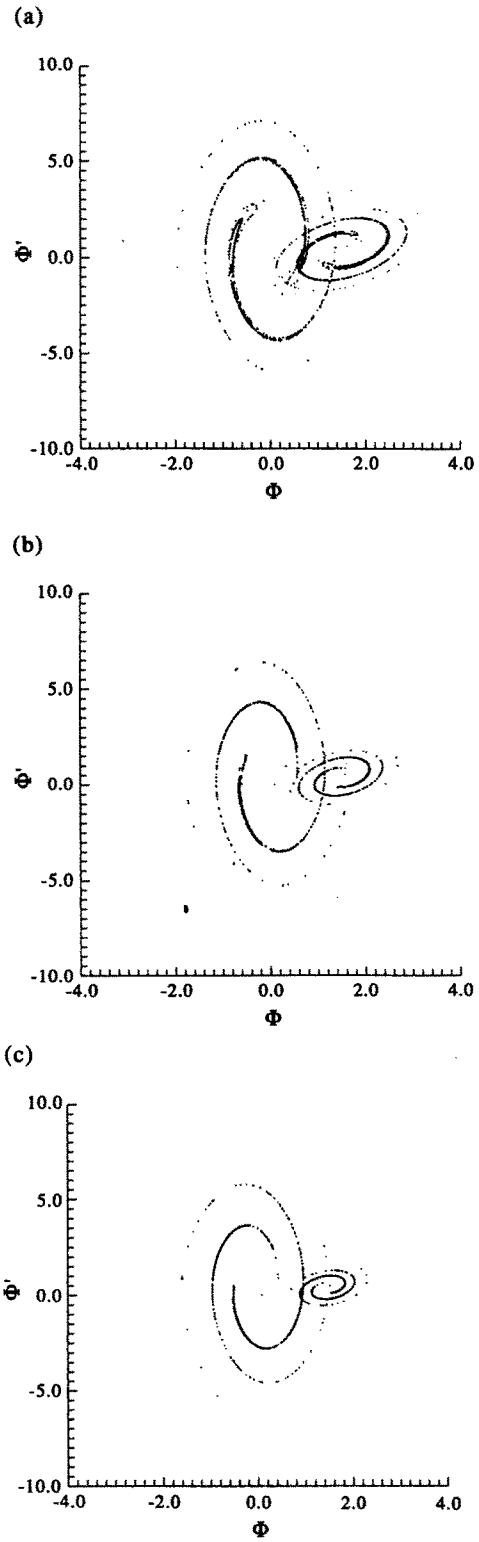

Fig. 16. Poincaré maps for $D = 10$, $E = 10$, initial conditions (0.0873, 0.0) and (a) $C = 0.4$, (b) $C = 0.6$, and (c) $C = 0.8$.

Table 3. Lyapunov exponents λ_1 and λ_2, $\lambda_1+\lambda_2$ and λ_1 for $D = E = 10$ and $C = 0.0$, 0.2, 0.4, 0.6, and 0.8

C	D	E	λ_1	λ_2	$\lambda_1+\lambda_2$	d_1
0.0	10.0	10.0	0.3794	−0.3794	0.0	2
0.2	10.0	10.0	0.2397	−0.5283	−0.2886	1.454
0.4	10.0	10.0	0.1827	−0.7598	−0.5771	1.241
0.6	10.0	10.0	0.1388	−1.0044	−0.8656	1.138
0.8	10.0	10.0	0.1193	−1.2734	−1.1541	1.094

6. CONCLUSIONS

A few remarks can be made from the above discussions.

(1) Chaos happens when the parameter E, which is related to the angular velocity of circular motion and the length of the pendulum, is near or equal to 10.

(2) The system without damping becomes chaotic by a quasi-periodic route. When the system is in quasi-periodic motion, its Poincaré map is composed of two closed curves, which move further apart when the parameter D, the ratio of the radius of the circular motion to the length of the pendulum, increases. When the system is in chaotic motion, the points on the Poincaré map are distributed uniformally and its dimension is two. But there is no strange attractor on the map. For the chaotic motion, the Lyapunov exponent λ_1 is equal to $-\lambda_2$ and becomes larger as D increases. Different initial conditions could get the same Poincaré map for chaotic motions.

(3) The system with damping becomes chaotic by a periodic-doubling route. The interval between the bifurcation points becomes smaller as the parameter D increases. When the system is in periodic motion, the Poincaré map consists of only a finite set of points. When the system is in chaotic motion, the points on the Poincaré map are not distributed uniformally and form a strange attractor with two similar patterns of different size. The dimension of the strange attractor is between one and two, and it becomes larger when D increases. Different initial conditions could also get the same Poincaré map for chaotic motions.

(4) The amplitude probability distribution, which is found to be feasible for predicting chaos, is continuous for both quasi-periodic and chaotic motions. The range of the amplitude for chaotic motion is from $-\pi$ to π, but smaller for quasi-periodic motion. The amplitude probability distribution for periodic motion is discrete. Therefore, the amplitude probability distribution can also be used as a method to diagnose whether the motion is regular or chaotic. For chaotic motion, the amplitude probability distribution is found to be very sensitive to the initial conditions.

(5) When the parameter E is fixed, chaos happens at larger D if the damping increases.

(6) With the angular velocity of the circular motion and the geometry being fixed, the fractal dimension of the strange attractor becomes smaller when the damping increases.

If the behavior of a system can be predicted, then the designed device will be safer and more reliable. Because of the unpredictability and sensitivity to changes in initial conditions of chaotic motion, engineers had better avoid using the parameters in the equation of motion which will lead to chaos. Therefore, before establishing a physical system, numerical simulations to see whether the system will be chaotic are suggested. It is also important to indicate that damping could help suppress the occurrence of chaos.

REFERENCES

Farmer, J. D., Ott, E. and Yorke, J. A. (1983). The dimension of chaotic attractors. *Physica* **7D,** 153–180.

Frederickson, P., Kaplan, J. L., Yorke, E. D. and Yorke, J. A. (1983). The Lyapunov dimension of strange attractors. *J. Differential Equations* **49,** 185–207.

Gerald, C. F. and Wheatley, P. O. (1984). *Applied Numerical Analysis* (3rd Edn). Addison-Wesley, Massachusetts.
Jensen, R. V. (1987). Classical chaos. *American Scientist* **75**, 168–181.
Panayotidi, T. and DiMaggio, F. (1988). Pendulum with support in circular orbit. *ASCE J. Engng Mech.* **114**(3), 478–498.
Yeh, J. and DiMaggio, F. (1991). Chaotic motion of pendulum with support in circular orbit. *ASCE J. Engng Mech.* **117**(2), 329–347.